Tikrit Journal of Engineering Sciences

TJES Tikrit Journal of Engineering Sciences

Open Access

Article

Numerical Investigation of the Effect of Post Notching Size and Location on the Behavior of Reinforced Concrete Beam before and after Strengthening

Harith Al-Salman [1], Hassanin Abd Ali Alfatlawy [2], Zainb Kareem Al-Mamory [3], Hayder Abdulwahid Khalaf [3], Fuad Abutaha [4]

[1] Civil Department, Engineering College, Babylon University, Babil, Iraq.
[2] Civil Department, Engineering College, Kerbala University, Karbala, Iraq.
[3] Civil Department, Engineering College, Baghdad University, Baghdad, Iraq.
[4] Civil Department, Engineering College, Antalya Bilim University, Antalya,Turkey.

Emails:
Harith Al-Salman : eng.harith.amer@uobabylon.edu.iq , Hassanin Abd Ali Alfatlawy : hassanin.a@uokerbala.edu.iq ,
Zainb Kareem Al-Mamory : z.abd1901m@coeng.uobaghdad.edu.iq , Hayder Abdul wahid Khalaf : h.khalaf1001@coeng.uobaghdad.edu.iq ,
Fuad Abutaha : fuad.abutaha@antalya.edu.tr

Abstract:

Some structural concrete projects suffered from post-casting changes or modifications to accommodate pipe services due to inefficient initial planning or management. This study aims to evaluate the performance of a reinforced concrete beam with dimensions of 300 mm x 600 mm x 3800 mm for width, height, and span length, respectively. Notches were made at various locations on the face of the support, with various notch depths. A nonlinear parametric three-dimensional (3D) finite element model was developed in Abaqus to evaluate the structural behavior of models subjected to notching with a fixed width of about 150 mm and a length equal to the beam width (or 300 mm). The study covered two main parameters: notch locations at three distances from the face of support (1d,2d, and 3d), and notch depth (0.5d and 0.75 d). Several parameters were adopted as evaluation criteria, including maximum load-carrying capacity, stiffness, ductility, and toughness. Results revealed that the most critical location occurs when the notch distance is three times the beam's clear span, compared to other cases. Also, a notch depth of 0.75d in some locations has a slight effect compared with a notch depth of 0.5d. A steel strip jacket was introduced as an enhancement modification, with a specific configuration for all studied parameters, and showed comparable efficiency to the unnotched beam model.

Keywords:

Notched beam; Abaqus; FEM; Toughness; Ductility; Stiffness; Concrete damaged plasticity.

Highlights:

- FEA models evaluate notch size and location effects on RC beam performance.
- Notch location at 3d from support identified as the most critical for stability.
- Deeper notches significantly reduce load capacity, stiffness, and ductility.
- Steel strip jackets effectively restore capacity and stiffness of notched beams.

Citation:

Al-Salman H, Ali Alfatlawy HA, Al-Mamory ZK, Khalaf HA, Abutaha F. **Numerical Investigation of the Effect of Post Notching Size and Location on the Behavior of Reinforced Concrete Beam before and after Strengthening**. *Tikrit Journal of Engineering Sciences* 2026; **33**(1): 2380.

Article History:

Received:	13	Oct.	2024
Received in revised form:	26	Dec.	2024
Accepted:	27	Feb.	2025
Final Proofreading:	20	Jan.	2026
Available online:	06	May	2026

https://doi.org/10.25130/tjes.33.1.12

Corresponding Author*:

Harith Al-Salman
Civil Department, Engineering College, Babylon University, Babil, Iraq.
Email: eng.harith.amer@uobabylon.edu.iq

1.INTRODUCTION

A beam with a notch is a structural component with a cutout or indentation along its length [1]. The notch is typically created to accommodate other structural elements, such as pipes, ducts, or cables, that need to pass through the beam. The presence of a notch in the beam can significantly affect its strength and load-bearing capacity, as it creates stress concentrations at the notch corners [2]. Therefore, engineers and architects need to carefully design and analyze notched beams to ensure that they can withstand the expected loads and stresses [3]. In this context, factors such as the size and location of the notch, the beam's material properties, and the type of loading it will be subjected to all need to be taken into consideration [4, 5]. Despite the challenges associated with notched beams, they can provide an efficient, space-saving solution in many construction projects, enabling the integration of multiple systems and components within limited space. Certainly! Notched beams are often used in construction projects where space is limited, such as in high-rise buildings, bridges, and tunnels. By creating a notch in the beam, other structural elements can be integrated into the same area, saving valuable space [6]. For example, a notched beam may be used to support an HVAC duct or electrical conduit, allowing these systems to run through the beam rather than around it [7]. This can be particularly useful in applications where space is at a premium, such as in urban areas or in retrofit projects. However, a notch in a beam can also significantly reduce its strength and load-bearing capacity [8]. The corners of the notch create stress concentrations, where the material is more likely to fail under load [9]. To mitigate this effect, engineers use a variety of techniques, including fillet radii, chamfers, and reinforcement, to distribute stresses more evenly [10]. These techniques can help ensure the notched beam withstands the expected loads and stresses without failing. In addition to the challenges associated with designing and analyzing notched beams, manufacturing considerations must also be taken into account. Creating a notch in a beam can be complex, particularly for larger or more complex notches [11]. Specialized cutting and shaping tools may be required, and the process must be carefully controlled to ensure that the notch is created to the correct specifications [12]. Despite these challenges, notched beams can provide an efficient and effective solution in many construction applications, enabling the integration of multiple systems and components within limited space [13]. With careful design and analysis, notched beams can be used to create strong, reliable structures that meet the needs of modern construction projects [14]. Experimental studies about the methods of strengthening and repairing RC beams include the use of CFRP laminate and sheet, near-surface carbon fiber (SNSM-CFRP) strips, near-surface glass fiber (NSM-GFRP) rods, fiber reinforced concrete (FRC), reinforced concrete (RC) jacketing, sprayed fiber reinforced polymer FRP, epoxy injection, mortar jackets, CFRP laminate, and ultra-high-performance concrete (UHPC) layer. Every technique covered demonstrated that the reinforced and repaired beams' overall behaviour has improved, with their maximum load and ductility increasing as well [15]. To strengthen concrete beams against opening mechanism fracture failure, a steel channel plate was installed at the head of a notch. According to the test results, channel steel plate measures can increase the beam load capacity. The final failure of the reinforced concrete beams was caused by matrix cracking and interface debonding [1]. The interfacial stress was calculated using a mixed-mode cohesive law in the finite element simulation of notched steel beams reinforced with a CFRP plate. As the notch depth increased, the ultimate load and ductility significantly reduced. Additionally, while increasing the CFRP's thickness and elastic modulus increased bearing capacity, ductility declined, and early debonding failure was more likely [16]. Three-point bending tests were conducted on 24 notched beams with the strengthening system externally bonded to the bottom face of the beam to analyze bond behavior without the concrete's tensile input. Fiber-reinforced cementitious matrix (FRCM) systems with polybenzoxole (PBO) grid and cement-based mortar, as well as fiber-reinforced polymer (FRP) systems with carbon sheets and epoxy resin (CFRP), are the two systems under analysis. Peak load and ultimate displacement values for the conditioned specimens were comparable to those of the non-conditioned specimens, and the PBO-FRCM system was unaffected by environmental factors. The chosen test configuration on notched beams was utilised for the FRCM system, even though it was designed for the FRP system. The stress-global slip curve of the PBO grid–mortar matrix was evaluated using this test setup, which was based on some fundamental kinematics considerations underlying a rigid-body motion assumption after crack opening. The results showed that the curves obtained using the more popular single-lap or double-lap direct shear test setup reported in the literature were reasonably in agreement, both qualitatively and quantitatively. At 50 C, near the primer/epoxy's glass transition temperature, the CFRP system was sensitive to curing conditions. In contrast to the equivalent average load of the non-conditioned specimens, this curing condition resulted in a reduction in the average peak load of more than 30%, despite the relatively brief

application of this conditioning phase. There was no discernible decrease in the average peak load under the curing conditions at 30 C [17]. Three-point bending tests were conducted on ultra-high performance concrete UHPC notched beams to examine the impact of three notch-to-depth ratios of 1/6,1/3, and 1/2 at five different loading rates of 0.05, 0.50,1.25, 2.50, and 5.00 mm/min on flexural performance. The flexural characteristics of the UHPC notched beams are significantly impacted by loading rate and notch-to-depth ratio, according to test findings. The loading rate and the notch-to-depth ratio are found to boost the flexural strength. The loading rate increases the fracture energy, whereas the notch-to-depth ratio decreases it [18]. The extended finite element method (XFEM), the contour integral technique (CIT), and the virtual crack closure technique (VCCT) were the methods used. External post-tensioning (EPT), the shear span-to-depth ratio (S.S/D), and the initial notch-to-depth ratio (ao/D) were all the subject of a parametric research. Both XFEM and VCCT showed superior results; however, XFEM's flexural simulation was superior. On the other hand, the softening behaviour and the fracture path were not captured by the CIT models. Additionally, after lowering (ao/D) and S.S/D, the flexural capacity increased. Furthermore, employing EPT decreased flexural softening, demonstrated ductile flexural response, and enhanced flexural capacity [11]. FRP flexible sheets were used to retrofit the tension flanges with artificially notched mid-spans. The sheets were extended to cover portions of the beams, and varying-height webs were anticipated for the beams. Eleven box steel beams were tested under two-point loads up to failure; they included one undamaged beam, one damaged beam with a notch, and nine damaged beams with a notch that had been refitted with composite materials. The number of layers and the type of FRP (GFRP and CFRP) were considered. The results showed that attaching CFRP sheets to both the tension steel flange and a portion of the webs, rather than only the flange, improves the ultimate load of retrofitted beams, prevents debonding, and increases beam ductility [19]. A notched concrete beam repaired with cement mortar, bacterial mortar, and adhesive was also tested for flexural behaviour and performance. For all three repair materials, it was found that the repaired beam's ultimate load capacity was higher than that of the notched beam under consideration. Additionally, when glue was used to fix notched beams, the maximum ultimate load rose. Additionally, the bacterial mortar performed better in terms of the ultimate load than the cement mortar. It was discovered that using bacterial mortar to repair concrete constructions was more sustainable and long-lasting [20]. The primary purpose of this study is to investigate the behavior of reinforced concrete beams before and after notching. Various parameters, such as notch position and depth, were selected for this study and analysed numerically using nonlinear 3D modelling in the Abaqus environment (finite element software). The beams were then retrofitted with a steel jacket and compared with the reference (beam without notching) model.

2.RESEARCH METHODOLOGY

Twelve reinforced concrete beams, with and without notching, have a length, width, and depth of 3800, 300, and 600 mm, respectively, modelled and tested numerically as a fixed-support (the supporting length on both sides is 250 mm) beam under an incremental concentrated load at mid-span until failure. The design variables were the notching distance from the supports and the notching depth, as illustrated in Table 1 and Figs. 1-14. Three notch positions are evaluated: 1D from the support, 2D, and 3D. In addition, two notch depths are considered: 0.5D and 0.75D. Moreover, the notched beams are evaluated before and after enhancement using a steel jacket near the notch location. The dimensions and configurations of the steel jacket strips are illustrated in the figures previously mentioned. It is worth mentioning that the dimensions of the steel jacket were fixed for the simulated models.

Table 1 Details of Beams.

No.	Beam Mark	Description
1	RF	Reference beam without notching
2	1D-50	Beam with notching depth (0.5d) at (d) from support
3	1D-75	Beam with notching depth (0.75d) at (d) from support
4	1D-50-J	Beam with notching depth (0.5d) at (d) from support with jacket
5	1D-75-J	Beam with notching depth (0.75d) at (d) from support with jacket
6	2D-50	Beam with notching depth (0.5d) at (2d) from support
7	2D-75	Beam with notching depth (0.75d) at (2d) from support
8	2D-50-J	Beam with notching depth (0.5d) at (2d) from support with jacket
9	2D-75-J	Beam with notching depth (0.75d) at (2d) from support with jacket
10	3D-50	Beam with notching depth (0.5d) at (3d) from support
11	3D-75	Beam with notching depth (0.75d) at (3d) from support
12	3D-50-J	Beam with notching depth (0.5d) at (3d) from support with jacket
13	3D-75-J	Beam with notching depth (0.75d) at (3d) from support with jacket

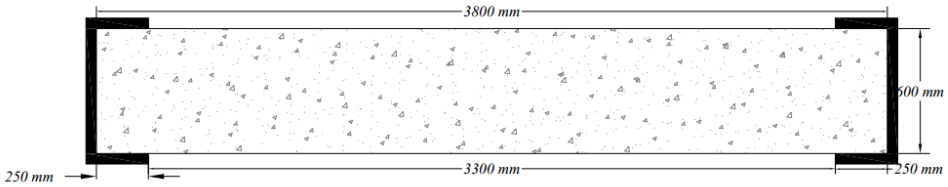

Fig. 1 Schematic Reference Beam without Notching

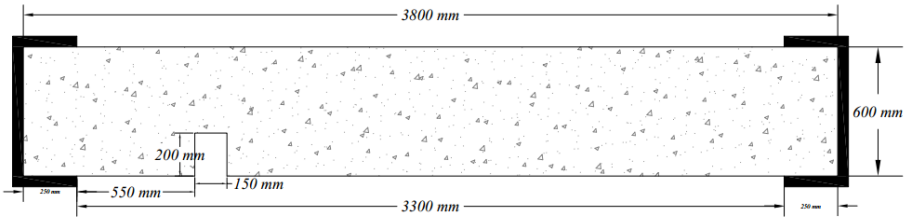

Fig. 2 Schematic Beam with Notching Depth (0.5d) at (d) from the Support.

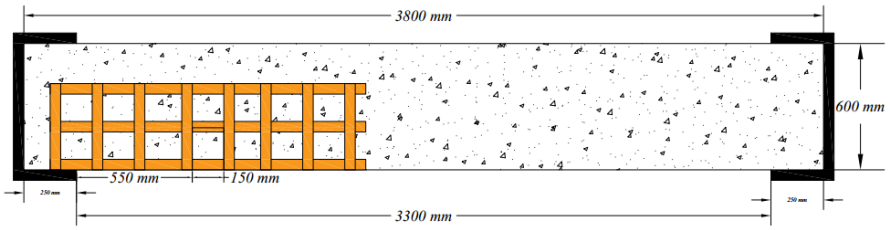

Fig. 3 Schematic Beam with Notching Depth (0.5d) at (d) from the Support with Jacket.

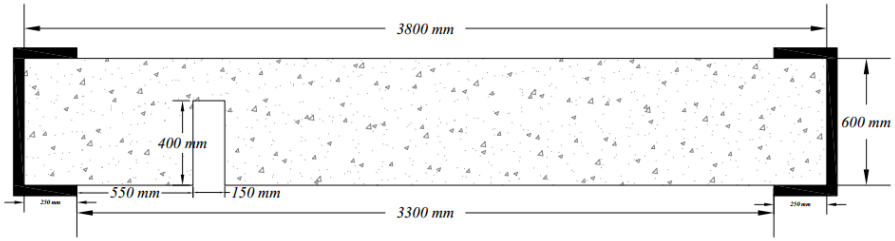

Fig. 4 Schematic Beam with Notching Depth (0.75d) at (d) from Support.

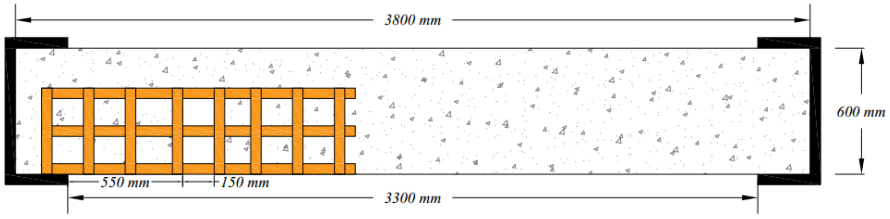

Fig. 5 Schematic Beam with Notching Depth (0.75d) at (d) from Support with Jacket.

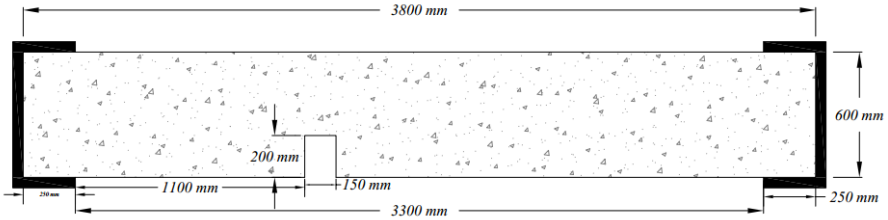

Fig. 6 Schematic Beam with Notching Depth (0.5d) at (2d) from Support.

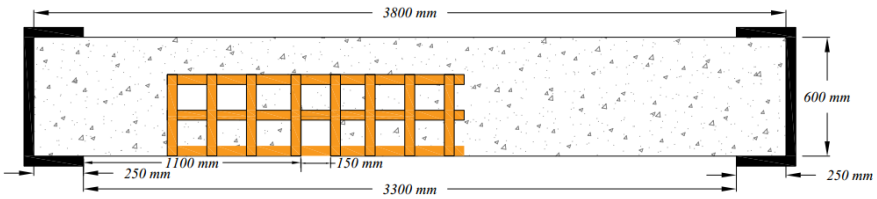

Fig. 7 Schematic Beam with Notching Depth (0.5d) at (2d) from Support with Jacket.

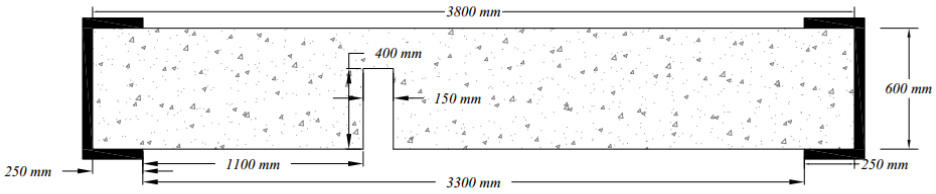

Fig. 8 Schematic Beam with Notching Depth (0.75d) at (2d) from Support.

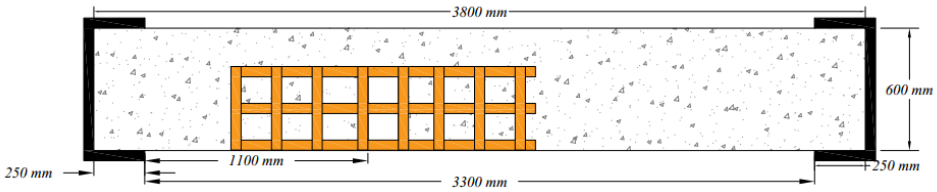

Fig. 9 Schematic Beam with Notching Depth (0.75d) at (2d) from Support with Jacket.

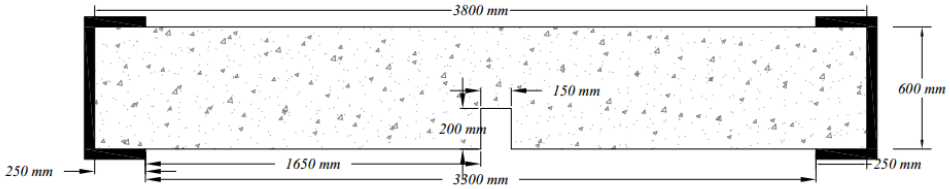

Fig. 10 Schematic Beam with Notching Depth (0.5d) at (3d) from Support.

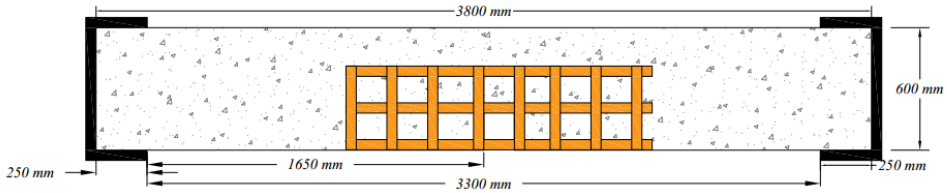

Fig. 11 Schematic Beam with Notching Depth (0.5d) at (3d) from Support with Jacket.

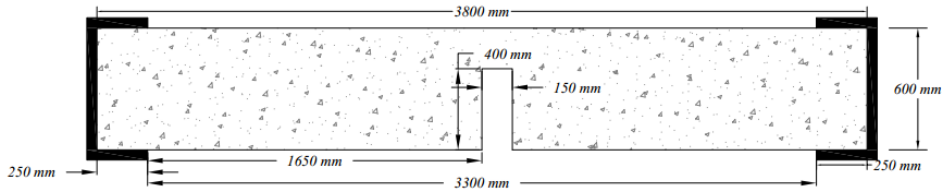

Fig. 12 Schematic Beam with Notching Depth (0.75d) at (3d) from Support.

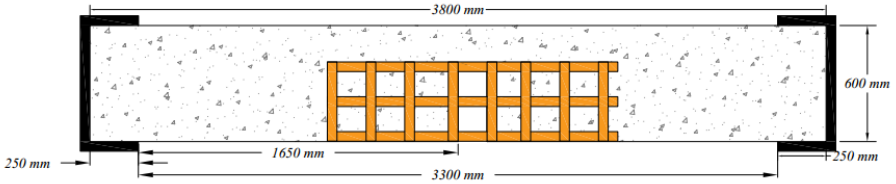

Fig. 13 Schematic Beam with Notching Depth (0.75d) at (3d) from Support with Jacket.

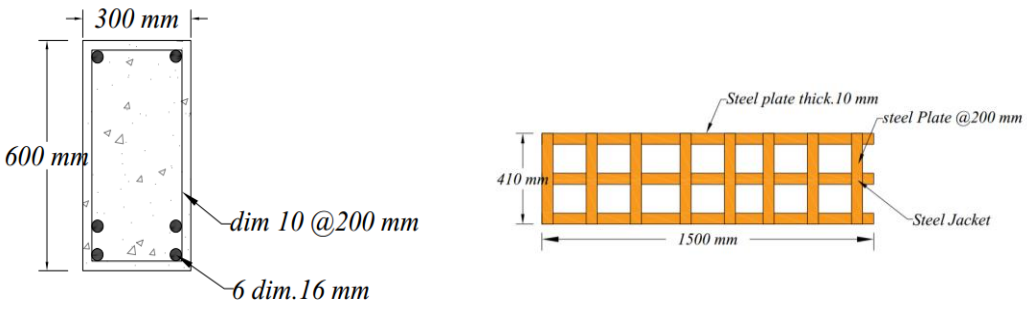

Fig. 14 Details of Steel Reinforcement and Steel Jacket.

3.NUMERICAL MODELLING USING THE FINITE ELEMENT METHOD

3.1.Numerical Validation and Mesh Sensitivity Analysis

To determine whether the numerical results are reliable, they must be validated and compared with experimental results to identify the relationship between the two in terms of a selected parameter. In this study, the validated experimental work for the concrete beam under the designation (B1) has been adopted for modelling and simulation [21]. The load-deflection curve behavior was assigned for comparison between the experimental and FEA models. Fig. 15 illustrates the concrete beam details subjected to four-point bending until failure. The beam dimensions are 100 mm x 150 mm x 1000 mm for width, height, and length, respectively. It is worth noting that the concrete strength class is regular concrete (30.3 MPa compressive strength), and the steel reinforcement bars are grade 60 (minimum yield strength of 420 MPa). The primary reinforcement includes two 10 mm diameter bars in the tension zone (bottom face) and shear reinforcement in the form of 6 mm diameter stirrups spaced at 50 mm.

The finite element modelling involved modelling the concrete beam and supports as 3D elements with the hexagonal, eight-nodes, reduced integration brick element (C3D8R), as shown in Fig. 16. While the reinforcement rebars were modelled as one-dimensional parts (1D) using the wire element library (element code: truss, T3D2). The concrete damaged plasticity (CDP) was used to define concrete material behavior, and elastic-perfect plastic behavior for steel reinforcement bars, with properties as reported in the adopted experimental work. The surface-to-surface interaction contact property between the load supports and the beam was assigned using two properties: normal and tangential behavior. The reinforcement steel bars were constrained within the concrete beam using embedded-region properties. The steel cylinder supports were assigned as rigid, non-deformable bodies to reduce simulation time and constrained using boundary condition properties to allow rotation perpendicular to the beam length. The displacement control method was used to apply the load on the top face of the simulated concrete beam, and the static analysis procedure was selected for the simulation.

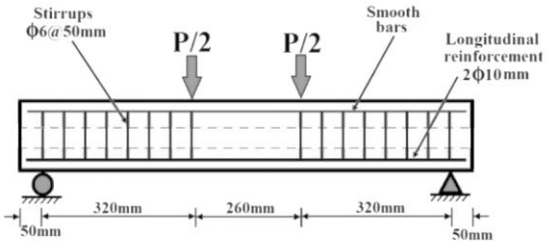

Fig.15 The Adopted Experimental Concrete Beam Details for Validation (B1 Specimen) [21].

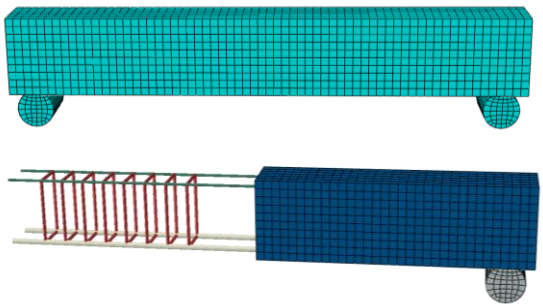

Fig. 16 Numerical Modelling and Meshing

3.1.1.Mesh Sensitivity Analysis

To make the simulation results independent of the mesh size on one side and reduce the time consumed during the analysis, a mesh sensitivity analysis and optimization were performed accordingly. Four different mesh sizes for the concrete beam were selected: 40 mm, 30 mm, 20 mm, and 10 mm, as shown in Fig. 17. The variation in the maximum load capacity of the beam was selected as the target optimization parameter. The result of the sensitivity analysis as illustrated in Fig. 18, has cleared that reducing the mesh size of the concrete beam resulted in reducing the maximum load carrying capacity significantly, up to specified a limit, where the variational in the max load decreased slightly after changing the size from 20 mm to 10 mm. thus, mesh size of 20 mm has been selected as optimum value since it balances the accuracy from a side, and time cost from another side.

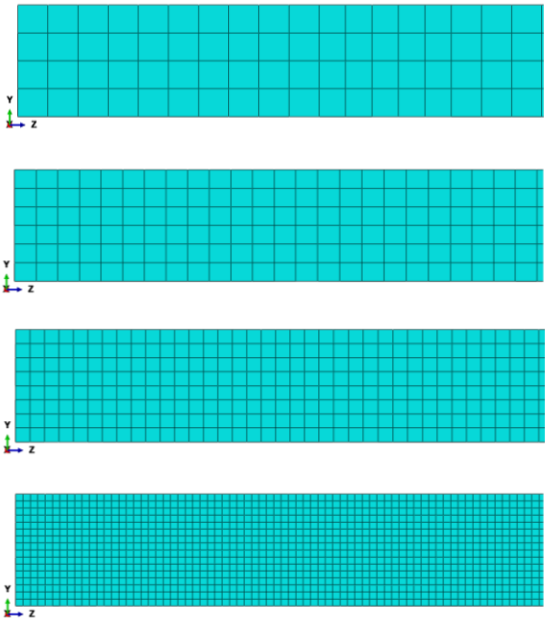

Fig.17 Various Concrete Beam Mesh Sizes for Sensitivity Analysis.

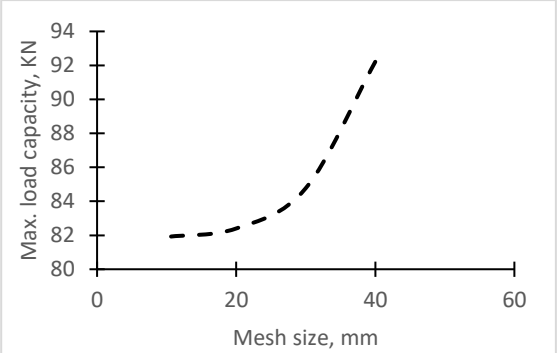

Fig. 18 Relation between Mesh Size and Beam Load Capacity.

3.2.Result of the Numerical Validation

After modelling the adopted experimental concrete beam in the Abaqus environment, the load vs. mid-span deflection curve was selected for validation, as indicated in Fig. 19. It can be noticed that the adopted configurations and parameters were able to predict a very close result compared to the experimental work, with an error percentage in the load capacity estimated by about 2%. In addition, the numerical curve behavior was similar to the adopted experimental work curve throughout all loading stages. Fig. 20 illustrates a visual inspection validation of the failure mode comparison between the experimental and numerical specimens. Thus, the numerical modelling successfully predicted the experimental results efficiently, and the assumed parameters can be adopted for further numerical modelling cases.

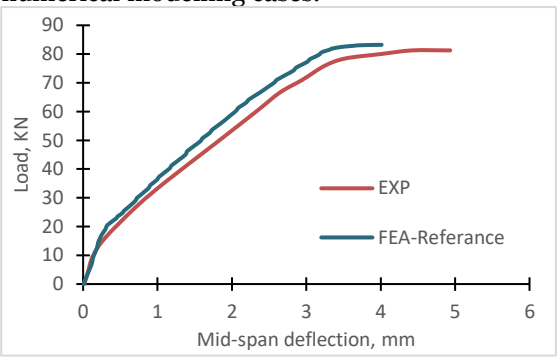

Fig. 19 Comparison between FEA Modelling and Experimental Work.

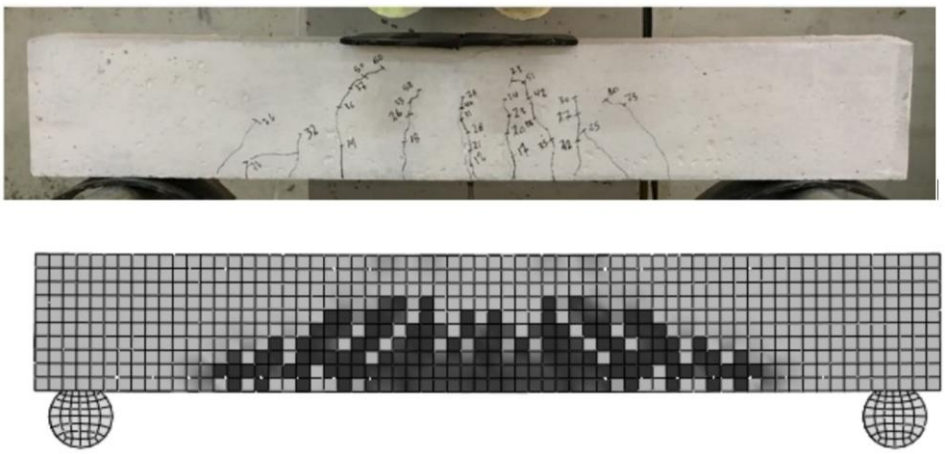

Fig. 20 Failure Mode Comparison between the Adopted Experimental Work and the FEM Modelling.

3.3.Material Behavior of Concrete and Steel Reinforcement of Simulated Notched Beams

All reinforced concrete beams were simulated by using the finite element package (ABAQUS/ standard) [22], which has the capability for modelling all types of linear and nonlinear problems. The behaviour of inelastic concrete was simulated using the concrete damage plasticity (CDP) approach [23], which is capable of simulating all types of reinforced and plain concrete structures [24]. The parameters of (CDP) were considered and illustrated in Table 2. For standard concrete, the dilatation angle ranges from 30 to 40 degrees, as reported in the Abaqus manual [22]. The recommended default eccentricity value, the ratio between biaxial compressive strength to initial uniaxial strength, and Kc values are 0.1, 1.16, and 0.66, respectively, in the same manner as reported by Abaqus documentation manual [22]. At the same time, the viscosity value can be calibrated by trial and error until suitable or acceptable results are achieved compared to the experimental work. The initial selected viscosity value of 0.0001 was selected to perform the simulation. The ABAQUS user manual has more details about the CDP approach [22]. The stress-strain relationship of uniaxial compressive for plain concrete after the elastic zone is presented in Fig. 21 (a). All reinforcement concrete beams were simulated by using the finite element- package (ABAQUS/ standard) [22], which has the capability for modelling all types of linear and nonlinear problems.

Table 2 Parameters of CDP.

Parameter	Value	Description
Dilation angle	35	The amount of the volume change to shear strain for reinforced concrete (30-40)
Eccentricity	0.1	The flow potential eccentricity, the default value is 0.1
biaxial to uniaxial strength ratio	1.16	The ratio between biaxial compressive strength and initial uniaxial strength ranges between 1.10 and 1.16
Kc	0.677	the ratio of the second stress invariant on the tensile meridian
Viscosity Parameter	0.0001	required when a convergence problem is caused by softening behavior

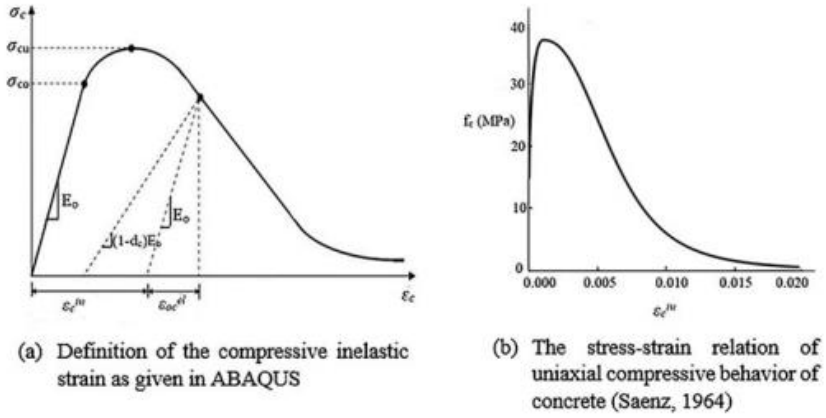

(a) Definition of the compressive inelastic strain as given in ABAQUS

(b) The stress-strain relation of uniaxial compressive behavior of concrete (Saenz, 1964)

Fig.21 Uniaxial Compressive Stress-Strain Relationship [22].

The relationship between stress and inelastic strain, as used in the finite element modelling of the uniaxial compressive behavior of concrete, is shown in Fig. 21 (b). In this study, a tension-softening response method in ABAQUS was used [22]. The uniaxial tension stress is shown in Fig. 22 (a). Fig. 22 (b) shows the stress-strain curves for the compressive strength of concrete (30 MPa) and the tensile behavior adopted in the study. Bilinear simulations are used to model steel reinforcement behavior based on the Von Mises failure approach. According to this definition, the stress-strain relation of reinforcing steel is perfectly elastic-plastic, as shown in Fig. 23. It is worth mentioning that the steel reinforcement bars of a grade of 60 (yield strength of 490 MPa) were used in this research work, while 300 MPa yield strength was identified for the steel jacket

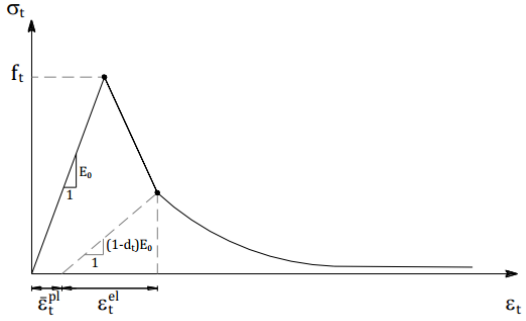

(a)

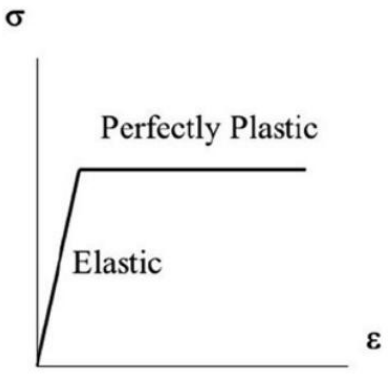

(b)

Fig.22 (a): Stress-Cracking Strain Curve for Concrete Tensile Behavior. (B): the Stress- Strain Relation of Reinforcing Steel Used in the Study [22].

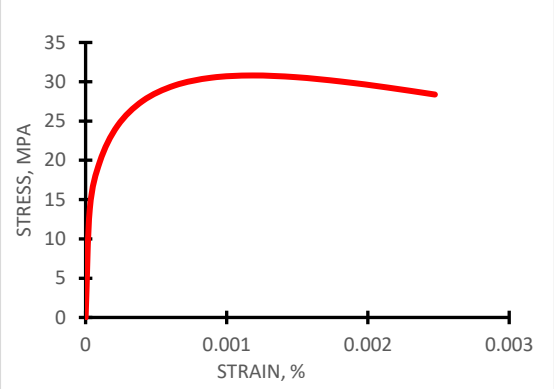

(a)

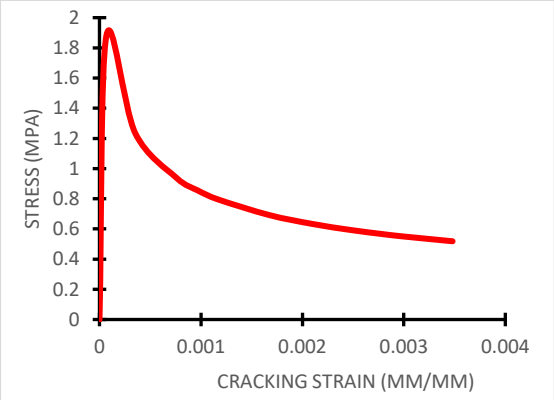

(b)

Fig. 23 Concrete Uniaxial Compressive (a) and Tensile (b) Stress-Strain Curves Adopted in the Study.

3.4.Element Type, Boundary Condition, and Loading Condition of the Notched Specimens

The reinforced concrete beams, with and without notching, and the steel jacket are simulated in 3D, except reinforcing bars are modelled as 3D stress elements. An 8-node linear brick (C3D8R) is used to simulate concrete beams and a steel jacket, while three degrees of freedom are used with a linear 3D two-node truss element (T3D2) to simulate reinforcing steel. Steel bars reinforcement of grade 60 (yield strength of 490 MPa) is constrained by being embedded in the concrete and a perfect bond between them (no slip between reinforcing bar and concrete), whereas the steel jacket is constrained by the type of tie with the concrete beam. Fig. 24 shows a steel reinforcement cage and a steel jacket. All finite element types used in this study are presented in Table 3. Boundary conditions of the reinforced concrete beams were simulated at the right and left ends by constraining the area (250 x 300 mm) in the x-,y-, and z- directions (i.e., U1=U2=U3=UR1=UR2=UR3=0). Displacement control at mid-span was used to simulate the applied load on the reinforced concrete beams and obtain the failure load. The boundary and loading conditions are illustrated in Fig. 25.

3.5.Mesh and Analysis of the Models

The selected optimal maximum element length of about 20 mm for the hexagonal element was adopted in this simulation. It is worth noting that the element size significantly affects the behaviour of the modelled beams and depends on the size of the concrete aggregates. The mesh of the simulated beams is presented in Fig. 26. Finite element software allows selection of the required analysis form, with the option of specifying step increments (fixed or automatic). In this study, the static analysis procedure type and automatic step increment are utilized.

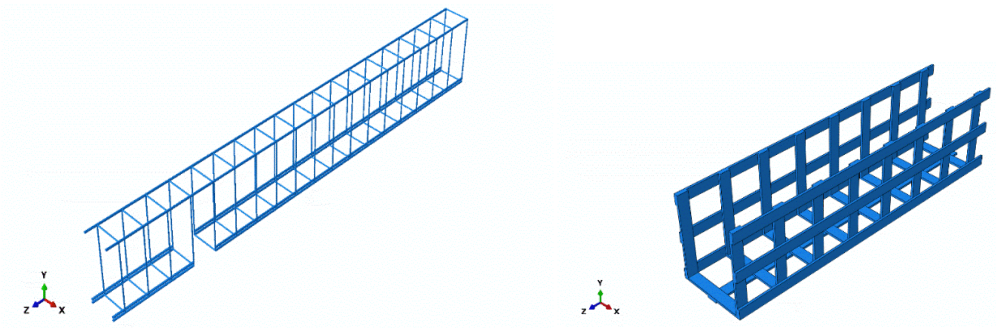

Fig. 24 Steel Reinforcement Cage and Steel Jacket.

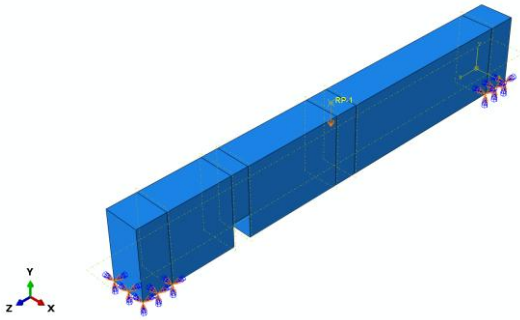

Fig. 25 The Boundary and Loading Condition.

Table 3 Description Elements.

Beam mechanisms	Family	Element Characteristics
Concrete and steel Jacket	3D-stress	C3D8R: 8-node linear brick, reduced integration
steel reinforcement	Truss	T3D2: 2-node linear 3D truss

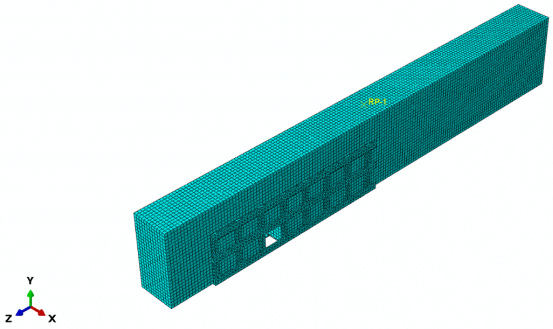

Fig. 26 Meshing Technology of the Modelled Beams.

4.RESULTS AND DISSECTION

4.1.*Behavior of Reinforced Concrete Notched Beam Models before Enhancement*

Figures 27 and 28 illustrate the effect of notch distance at three locations (1D, 2D, and 3D) and notch depths of about 0.5D and 0.75D from the face of the support. From the first view, it can be observed that the performance of a model in terms of load-displacement behaviour deteriorates, with ductility and stiffness degradation and absorbed energy highly affected as the notch location approaches the beam midspan, resulting in a significant reduction in the overall performance indices.

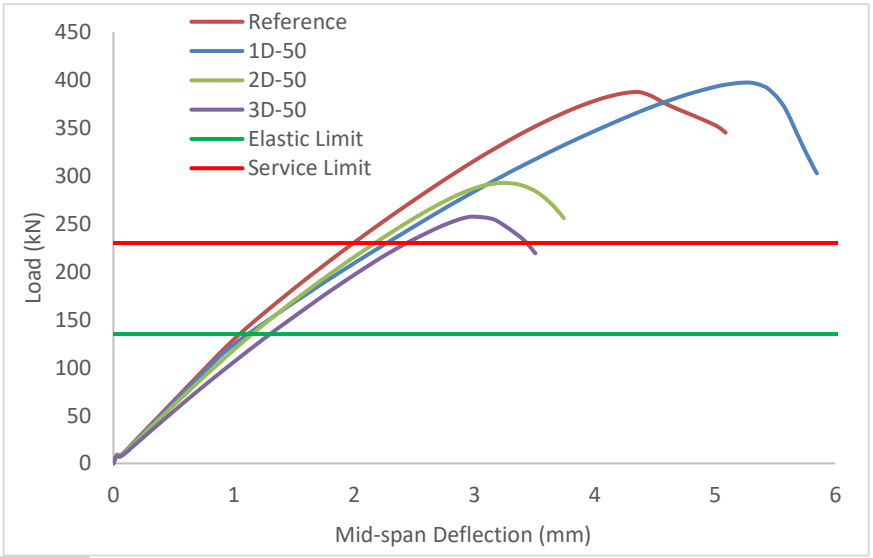

Fig. 27 Load vs Mid-Span Deflection for Beams with 50 mm Notch Depth.

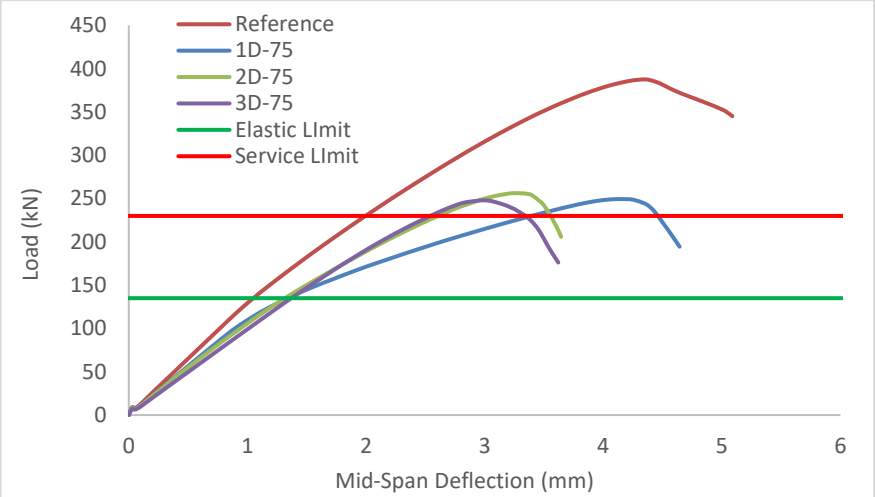

Fig. 28 Load vs Mid-Span Deflection for Beams with 75 mm Notch Depth.

For models with a notch depth of about 0.5D, in terms of load-carrying capacity, it can be observed in Fig. 29 that the maximum load decreased by about 8%, 24%, and 34%, respectively, for models 1D-ND0.5, 2D-ND0.5, and 3D-ND0.5, compared with the reference model. From the exact Figure, the maximum sustained load decreased by about 36%, 34%, and 64%, respectively, for models 1D-ND0.75, 2D-ND0.75, and 3D-ND0.75 compared with the reference model. Moreover, as the notch location approaches the midspan of the beam, the notch depth becomes insignificant, since the reduction values are approximately the same. Also, it can be observed that the variance in the load-carrying capacity increased dramatically as the notch location approached the midspan of the beam, reaching the same load-carrying capacity at location 3D. On the other hand, as illustrated in Fig. 30, the displacement at failure decreased proportionally as the notch location approached the beam midspan. The exact Figure shows that the displacements were approximately the same for models with the exact notch location and different notch depths.

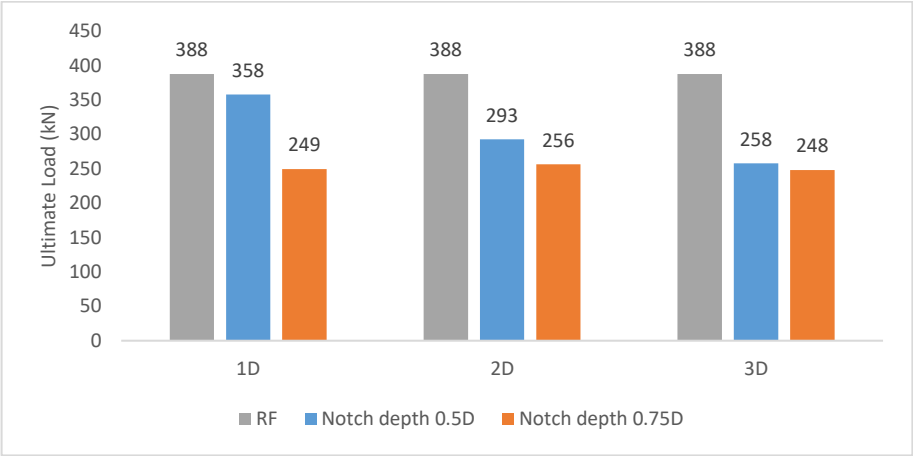

Fig. 29 The Ultimate Load-Carrying Capacity of Various Beams.

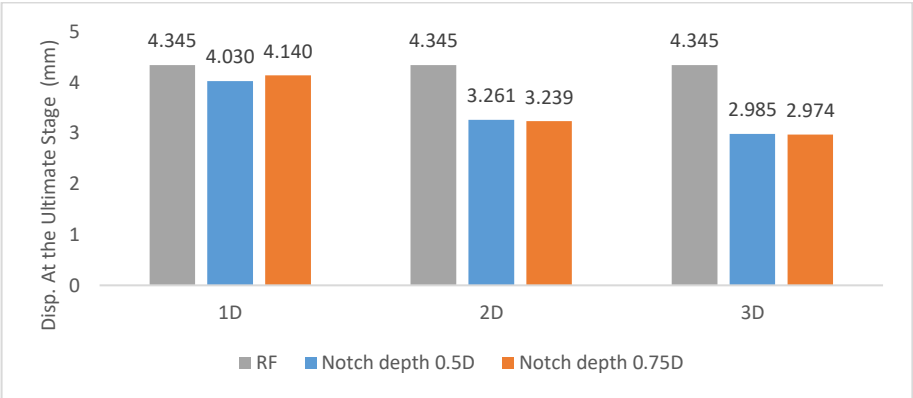

Fig. 30 Mid-Span Deflection Corresponded to the Ultimate Load-Carrying Capacity of Beams.

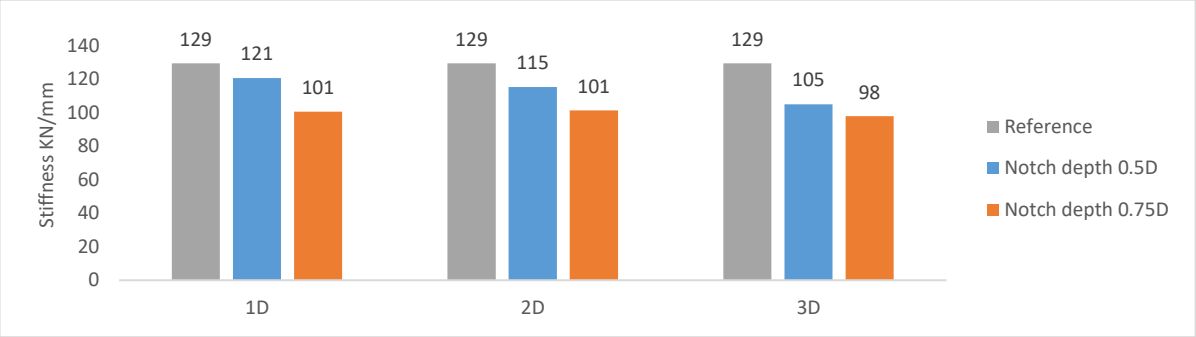

Fig. 31 The Initial Stiffness of Various Beam Models.

The elastic stiffness [26] (cracking load divided by the corresponding displacement) is an important index for measuring the structural efficiency of elements. From Fig. 31, it is clear that there is a noticeable reduction in stiffness as the notch depth increases or as the notch location approaches the centre. Also, the exact Figure shows that the stiffness variance of notched models with the exact location decreased with increasing notch distance from the support face. Overall, the stiffness decreased by about 7% and 22% at location 1D for depths of 0.5D and 0.75D, respectively. At the same time, the value was reduced by about 11% and 22% in the same manner when the notch location was at 2D. Finally, the reduction values were 19% and 24%, respectively, in the same comparison at location 3D.It can be clearly seen that models with a notch depth of 0.75D were not affected by the location, in contrast to those with a notch depth of 0.5D.In terms of the ductility index, this index indicates the ability of an element to withstand a load to a certain level, and the performance of the models was also evaluated [27]. The same was observed in the stiffness index: the notch depth was insignificant when the notch approached the beam centre. On the other side, it can be clearly observed that the ductility was reduced to half at such a location (3D) for both notch depths, which is considered the most critical location. The same observation can be made for the absorbed energy index, as illustrated in Fig. 32.In general, compared with the reference model, the ductility index of the models with a notch depth of 0.5D was reduced to 6%, 30%, and 44%, respectively, for notch locations 1D, 2D, and 3D. at the same time, the reduction values were about 44%, 42%, and 46% for models with a notch depth of 0.75D, in the same manner.The absorption energy index in KN.mm units, as illustrated in Fig.33, decreased with increasing notch depth from the side, up to the location at 3D, and decreased when the notch approached the centre of the beam from the other side. The most critical configuration was when the notch location was 3D from the beam face of the support and 0.75D deep, which was about 55%. while the lowest effect, about 13%, was for the notch configuration at 1D and 0.5D.

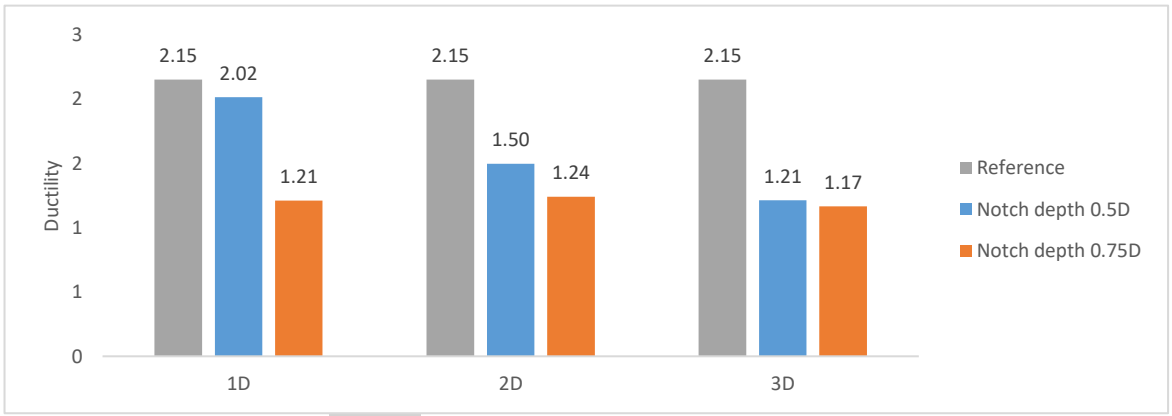

Fig. 32 Ductility Values of Various Beam Models.

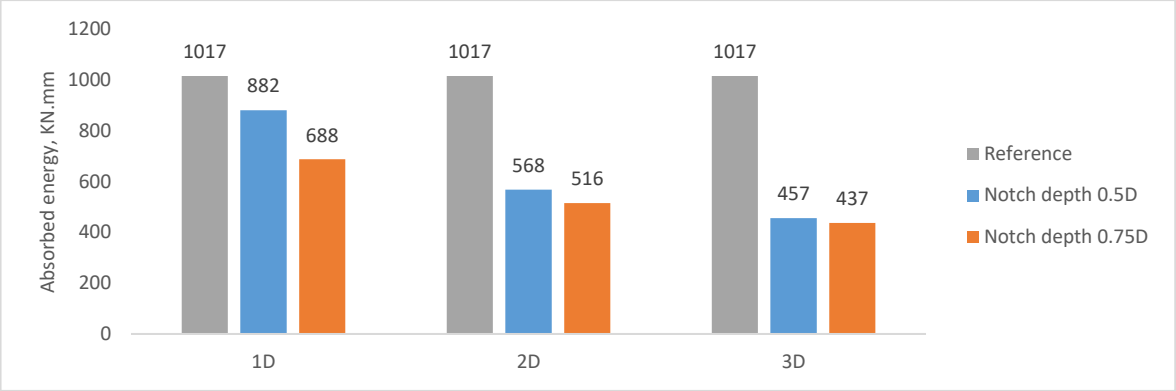

Fig. 33 The Absorption Energy Comparison of Various Modelled Beams.

4.2.Behavior of Reinforced Concrete Notched Beam Models after Enhancement

The study of the steel jacketing shows that such an enhancement or configuration can improve the beam's overall performance index, as illustrated in Figs. 34 and 35. In general, adopting such methodology has recovered the load-carrying capacity and comparable results to the reference beam (unnotched condition), as illustrated in Fig. 36. Also, the stiffness parameter results, as illustrated in Fig. 37, have shown that adopting such enhancement procedure resulted in comparable stiffness and sometimes the same as the reference value. The same explanation can be adopted for the ductility parameter, as clarified in Fig. 38. While Fig. 39 shows that the absorbed energy parameter for some enhanced models is higher than the reference value, other models have shown absorbed energy comparable to, and approximately the same as, the reference models.

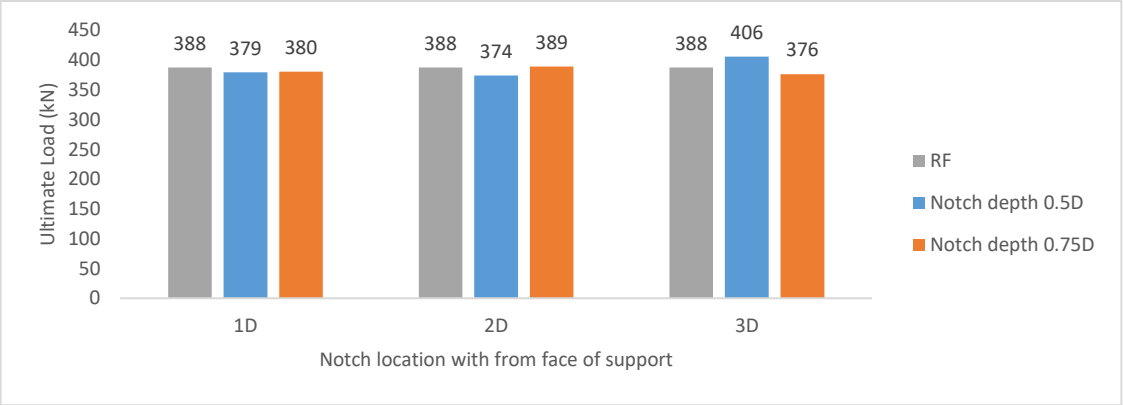

Fig. 34 The Ultimate Load-Carrying Capacity of the Beams after Enhancement.

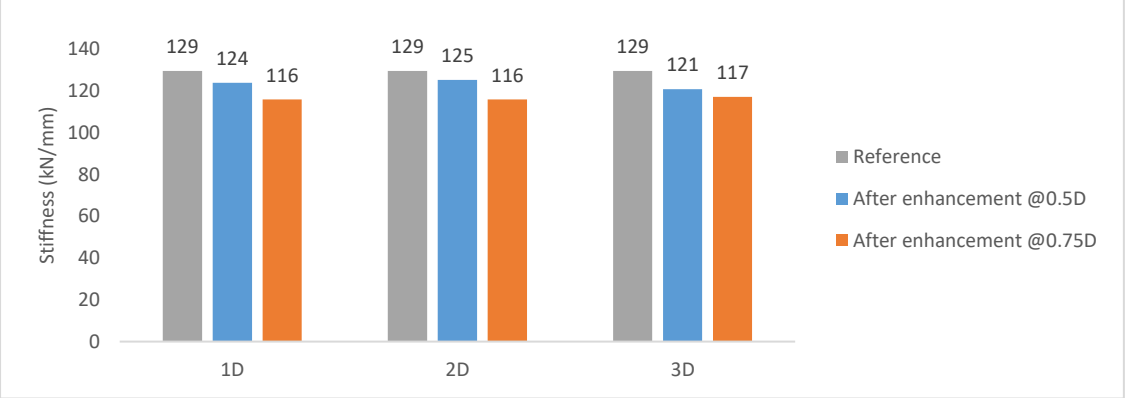

Fig. 35 The Initial Stiffness of Various Beam Models after Enhancement.

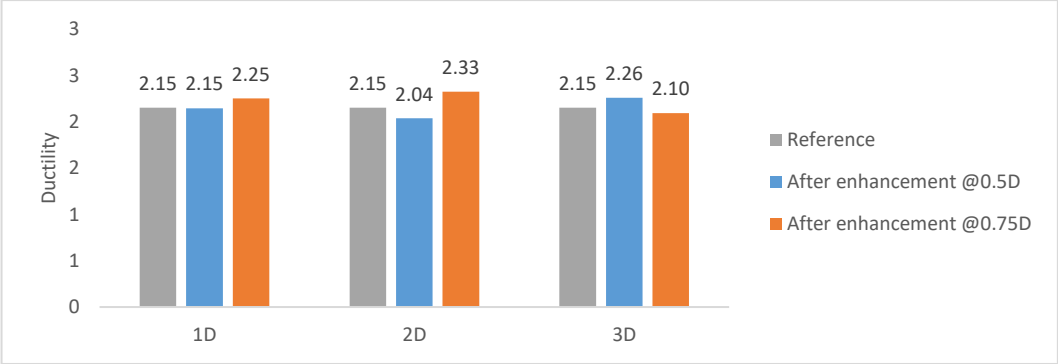

Fig. 36 Ductility Values of Various Beam Models after Enhancement.

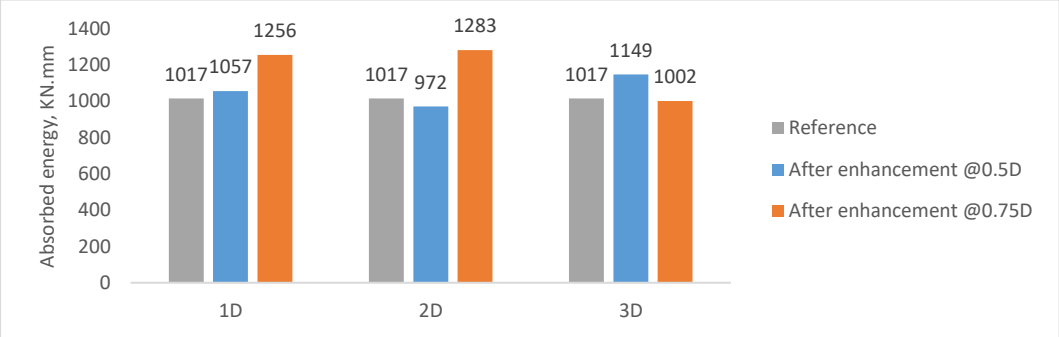

Fig. 37 The Absorption Energy Comparison of Various Modelled Beams after Enhancement.

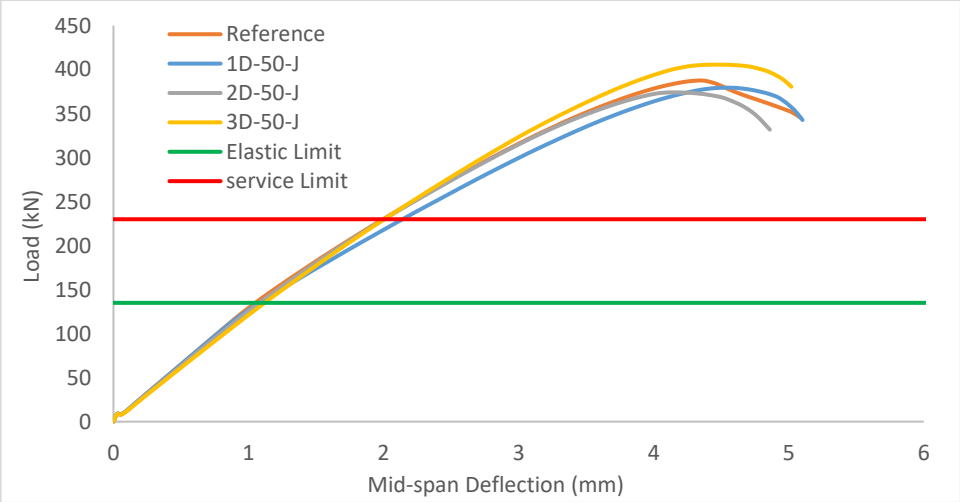

Fig. 38 Compares Mid-Span Deflection Values Corresponding to the Ultimate Load Capacity at Various (50 mm) Notch Locations.

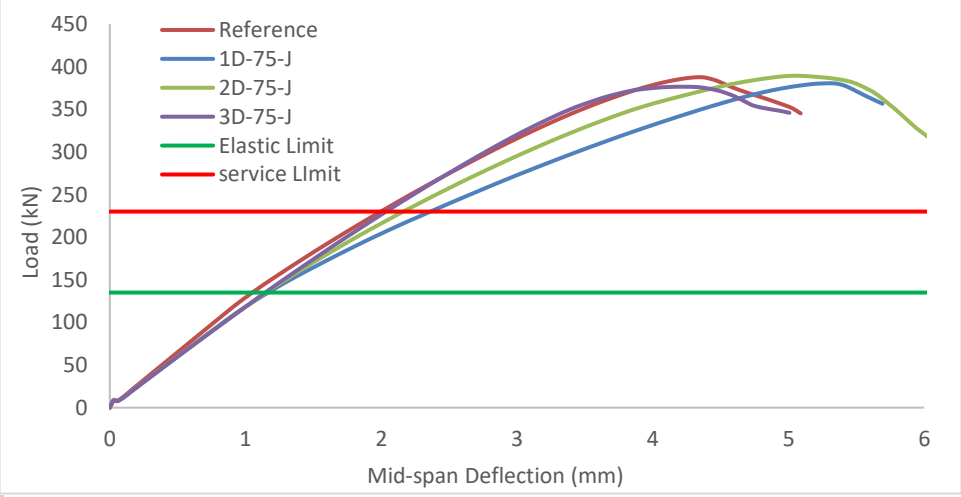

Fig. 39 Comparing the Ultimate Load Capacity of the Modeled Beams at Various (75 mm) Notch Locations.

The tensile crack patterns before and after enhancement are shown in Fig. 40. It can be noticed that the suggested enhancement configuration can help the notched beam restore its capacity by transferring stresses through the steel jacket, which works as a stress-transfer bridge device and avoids the weak region. Crack distribution away from the notch corners indicates that the steel jacket effectively transferred the stresses, converting the failure from a local phenomenon to its natural form (flexural crack). When the notch is located at 1D, it can be observed that a flexural crack, in addition to cracks near the notch corners, has appeared. Increasing the notch distance reduced flexural stresses and cracks at the beam's mid-span from the side, and densified the crack pattern near the notch corners. While with extra notch distance reaching near the mid-span (3D), no crack appeared in the flexural zone or mid-span location, only near the notch top corners. As shown in the Figure, Strengthening using a steel jacket method was effective in reducing or eliminating stress concentrations near or at notch corners, which are the leading cause and initial location of crack propagation throughout the concrete beam. By means of visual inspection, the increase in crack distribution in areas where strengthening was applied indicates the evident adoption of the steel jacket's efficiency in transferring stresses away from the notch location.

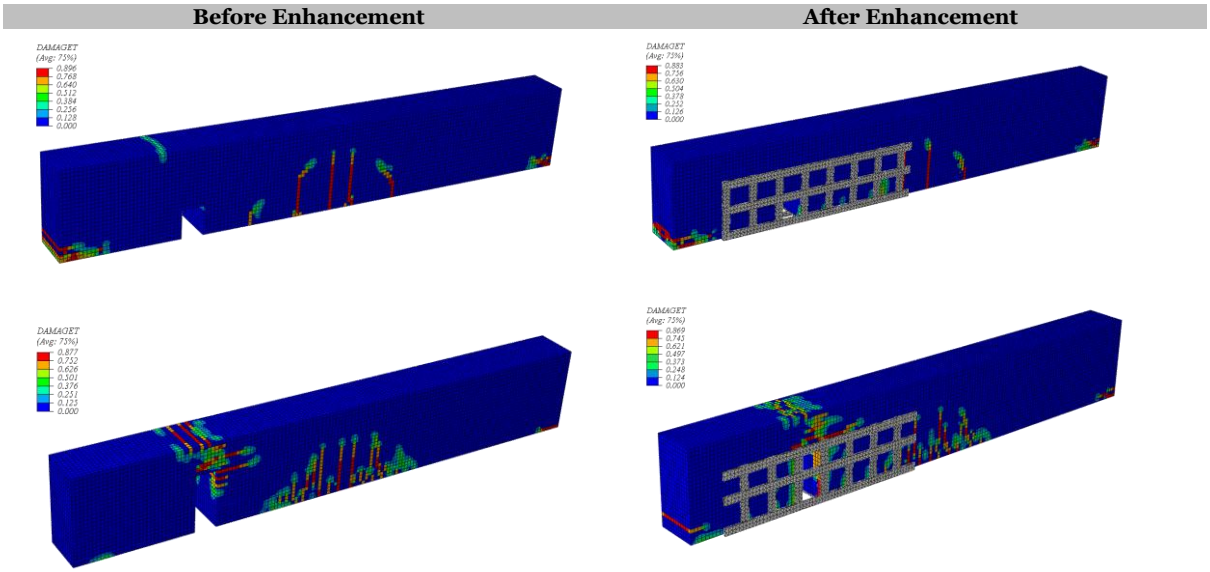

Notch at a Position Equal to 1D from the Support

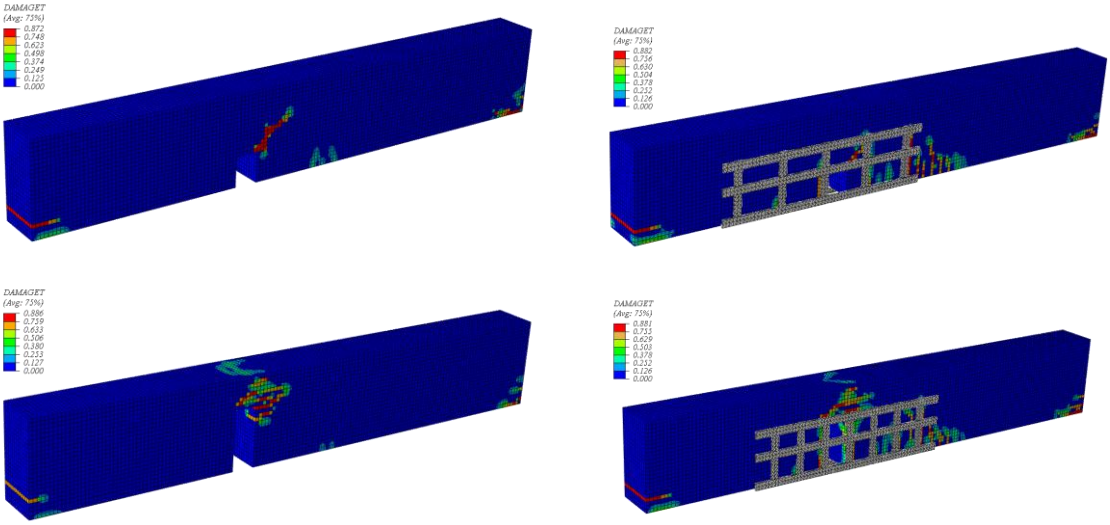

Notch at a Position Equal to 2D from the Support

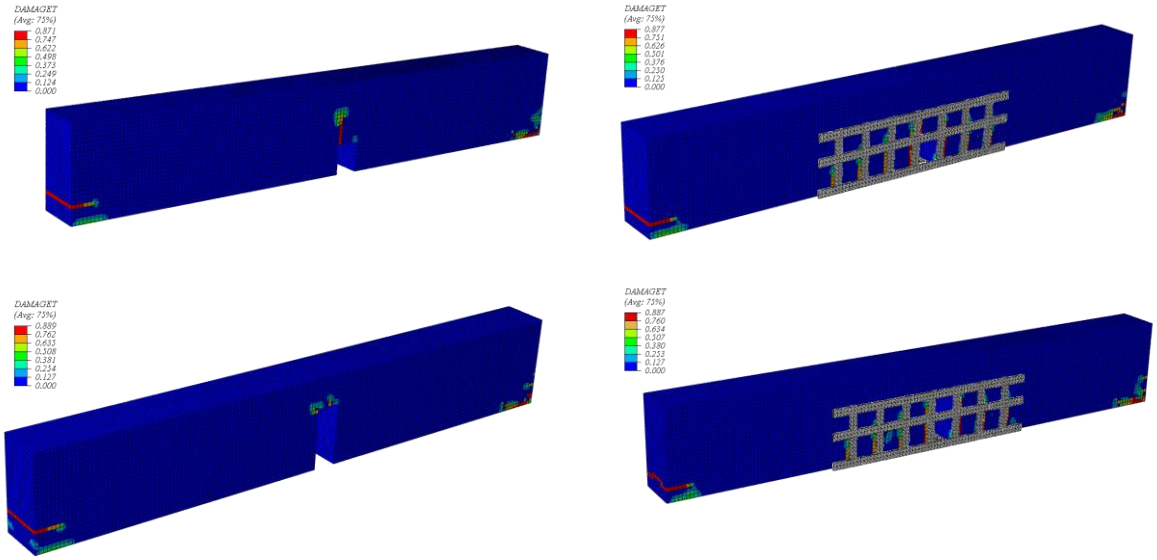

Notch at a Position Equal to 3D from the Support

Fig. 40 Cracks Pattern of the Simulated Beams before and after Enhancement for Notch Positions 1D, 2D, and 3D from the Support.

4.CONCLUSIONS

This research aims to identify and characterize notched-damage concrete beams before and after strengthening with a steel jacket. According to the numerical results, the main findings of the present study could be summarized as follows:

- As the notch site approaches the beam's midspan and reaches the same load capacity at point 3D, it is evident that the variation in load-bearing capacity is significant.
- The displacement at failure was more affected by notch location than by notch depth; thus, the displacement decreased proportionally as the notch location approached the beam midspan.
- The ductility index of the models with 0.5D and 0.75D notch depths was generally lower than that of the reference model.
- The absorption energy index decreased as the notch moved deeper from the side towards the 3D position, and it also decreased as the notch moved towards the beam's center from the opposite side.
- The suggested improvement can restore the overall bending performance index of the beam, as shown in research on steel jacketing. The adopted methodology and methods for strengthening were successful in restoring the concrete beam's bending strength efficiently. Thus, it is recommended that the suggested strengthening method be applied to repair damage to the concrete beam caused by accident notching in the future.

REFERENCES

[1] Zhong J, Zhou Y, Bao Q, Wang E, Li Q. **Strengthening Mechanism of Channel Steel Plate for Notched Concrete Beams Against Fracture: Test and Numerical Study.** *Engineering Fracture Mechanics* 2017; **180**: 132–147.

[2] Geers MGD, De Borst R, Peerlings RHJ. **Damage and Crack Modeling in Single-Edge and Double-Edge Notched Concrete Beams.** *Engineering Fracture Mechanics* 2000; **65**(2-3): 247–261.

[3] Marí A, Bairán J, Cladera A, Oller E, Ribas C. **Shear-Flexural Strength Mechanical Model for the Design and Assessment of Reinforced Concrete Beams.** *Structure and Infrastructure Engineering* 2015; **11**(11): 1399–1419.

[4] Kim H, Wagoner MP, Buttlar WG. **Micromechanical Fracture Modeling of Asphalt Concrete Using a Single-Edge Notched Beam Test.** *Materials and Structures* 2009; **42**(5): 677-689.

[5] Li X, He P, Tang J, Chen X. **Experimental and Numerical Studies on Fracture Characteristics of Notched Granite Beams under Cyclic Loading and Unloading.** *Journal of Strain Analysis for Engineering Design* 2021; **56**(1): 3-17.

[6] Benaoum F, Khelil F, Benhamena A. **Numerical Analysis of Reinforced Concrete Beams Pre-Cracked Reinforced by Composite Materials.** *Fracture and Structural Integrity* 2020; **14**(54): 282-296.

[7] Kantar E, Erdem RECEP, Anıl Ö. **Nonlinear Finite Element Analysis of Impact Behavior of Concrete Beam.** *Mathematical and Computational Applications* 2011; **16**(1): 183-193.

[8] Cotsovos DM, Zeris CA, Abbas AA. **Finite Element Modelling of Structural Concrete.** *2nd International Conference on Computational Methods in Structural Dynamics & Earthquake Engineering* 2009; Rodos, Greece: 1-21.

[9] Amiri S, Masoudnia R. **Investigation of the Opening Effects on the Behavior of Concrete Beams without Additional Reinforcement in Opening Region Using FEM Method.** *Australian Journal of Basic and Applied Sciences* 2011; **5**(5): 617-627.

[10] Archundia-Aranda HI, Tena-Colunga A, Grande-Vega A. **Behavior of Reinforced Concrete Haunched Beams Subjected to Cyclic Shear Loading.** *Engineering Structures* 2013; **49**: 27-42.

[11] Tawfik AB, Mahfouz SY, Taher SEDF. **Nonlinear ABAQUS Simulations for Notched Concrete Beams.** *Materials* 2021; **14**(23): 7349.

[12] Vecchio FJ, Collins MP. **The Modified Compression-Field Theory for Reinforced Concrete Elements Subjected to Shear.** *ACI Journal* 1986; **83**(2): 219-231.

[13] Benedetti L, Cervera M, Chiumenti M. **3D Numerical Modelling of Twisting Cracks under Bending and Torsion of Skew Notched Beams.** *Engineering Fracture Mechanics* 2017; **176**: 235-256.

[14] Zhong J, Song C, Xu J, Cheng Y, Liu F. **Experimental and Numerical Simulation Study on Failure Mode Transformation Law of Reinforced Concrete Beam under Impact Load.** *International Journal of Impact Engineering* 2023; **179**: 104645.

[15] Hassan RF, Latief AF. **Repairing and Strengthening Techniques of RC Beams: A Review.** *3rd International Conference for Civil Engineering Science (ICCES 2023)* 2023; Ad Diwaniyah, Iraq: 1-12.

[16] Deng J, Li J, Wang Y, Xie W. **Numerical Study on Notched Steel Beams Strengthened by CFRP Plates.** *Construction and Building Materials* 2018; **163**: 622-633.

[17] De Domenico D, Urso S, Borsellino C, Spinella N, Recupero A. **Bond Behavior and Ultimate Capacity of Notched Concrete Beams with Externally-Bonded FRP and PBO-FRCM Systems under Different Environmental Conditions.** *Construction and Building Materials* 2020; **265**: 121208.

[18] Meng W, Yao Y, Mobasher B, Khayat KH. **Effects of Loading Rate and Notch-to-Depth Ratio of Notched Beams on Flexural Performance of Ultra-High-Performance Concrete.** *Cement and Concrete Composites* 2017; **83**: 349-359.

[19] El-Taly B. **Structural Performance of Notch Damaged Steel Beams Repaired with Composite Materials.** *International Journal of Advanced Structural Engineering (IJASE)* 2016; **8**(2): 119-131.

[20] Khan W, Akhtar S, Rawat A, Basu A. **Experimental and Numerical Study on Flexural Behavior of Concrete Beams Using Notches and Repair Materials.** *Sustainability* 2024; **16**(7): 2723.

[21] Ismael MA, Hameed YM. **Structural Behavior of Hollow-Core Reinforced Self-Compacting Concrete Beams.** *SN Applied Sciences* 2022; **4**(5): 150.

[22] Dassault Systemes. **Abaqus Product Documentation: Abaqus Analysis User's Manual, Version 2021.** *Dassault Systèmes Provence* 2021.

[23] Raza A, Khan QUZ, Ahmad A. **Numerical Investigation of Load-Carrying Capacity of GFRP-Reinforced Rectangular Concrete Members Using CDP Model in ABAQUS.** *Advances in Civil Engineering* 2019; **2019**: 1745341.

[24] Al-Mamory ZK, Al-Ahmed AHA. **Behavior of Steel Fiber Reinforced Concrete Beams with CFRP Wrapped Lap Splice Bars.** *Structures* 2022; **44**: 1995-2011.

[25] Ibrahim FH, Ali AH. **Finite Element Analysis of Cracked One-Way Bubbled Slabs Strengthened by External Prestressed Strands.** *Journal of Engineering* 2021; **27**(1): 45-65.

[26] Muhtar, et al. **The Prediction of Stiffness of Bamboo-Reinforced Concrete Beams Using Experiment Data and Artificial Neural Networks (ANNs).** *Crystals* 2020; **10**(9): 757.

[27] Thamrin R, Zaidir Z, Iwanda D. **Ductility Estimation for Flexural Concrete Beams Longitudinally Reinforced with Hybrid FRP–Steel Bars.** *Polymers* 2022; **14**(5): 1017.